SIMULATION OF LASER WAKEFIELD ACCELERATION IN THE LORENTZ BOOSTED FRAME WITH UPIC-EMMA

Peicheng Yu*, Viktor K. Decyk, Weiming An, Frank S. Tsung, Warren B. Mori, UCLA, CA 90024
Xinlu Xu, Wei Lu, Tsinghua University, Beijing 100084, China
Jorge Vieira, Ricardo A. Fonseca, Luis O. Silva, Instituto Superior Técnico, Lisbon, Portugal

Abstract

Simulating Laser wakefield acceleration (LWFA) in a Lorentz boosted frame in which the plasma drifts towards the laser with v_b can speedup the simulation by factors of γ_b^2, where γ_b is the Lorentz factor of the boosted frame. To eliminate the high frequency numerical instability induced by relativistic plasma drift in these simulations, we develop a fully parallelized, multi-dimensional, particle-in-cell code that uses a spectral solver to advance the Maxwell's equations. This new EM-PIC code is called UPIC-EMMA and it is based on the components of the UCLA PIC framework (UPIC). It is shown that using UPIC-EMMA, LWFA simulations in the boosted frames with large γ_b can be conducted without any notable numerical instability. We also benchmark the UPIC-EMMA results with OSIRIS in the lab frame, an EM-PIC code with a finite difference time domain (FDTD) Maxwell solver, and good agreements are found.

INTRODUCTION

Laser wakefield acceleration [1] offers the potential to construct compact accelerators that has a numerous potential applications, and the last ten years has seen an explosion of theoretical and experimental results. Due to the strong nonlinear effects in the laser plasma interaction involved, numerical simulations, in particular particle-in-cell (PIC) simulation, are critical in exploring the physics of LWFA. Recently, it was shown that by performing the simulation in an optimal Lorentz boosted frame with velocity v_b, the time and space scales to be resolved in a numerical simulation may be minimized [2, 3, 4]. The basic idea is that in the boosted frame the plasma length (the laser propagation distance) is Lorentz contracted while the plasma wake wavelength and laser pulse length are Lorentz expanded, which lead to savings of factors of $\gamma_b^2 = (1 - v_b^2/c^2)^{-1}$ as compared to a lab frame simulation using the so-called moving window [5].

However, in the boosted frame simulations noise from a numerical instability can be an issue. As discussed in [6, 7, 8, 9, 10], the noise results from a numerical Cerenkov instability induced by the plasma drifting with relativistic speeds on the grid. According to the dispersion relation this numerical instability is attributed to the coupling between the wave-particle resonances with EM modes (including aliased modes) in the numerical system. The pattern of the instability in Fourier space can be found at the inter-

sections of the EM dispersion relation of the solver used in the simulation algorithm, and the wave-particle resonances [8, 9, 10].

In order to mitigate this instability, it is preferable to use an EM solver that eliminates the numerical instability at the main beam resonance [10]. When using a spectral solver that spatially advances the EM fields in Fourier space, its EM dispersion curve assures no instability pattern at the main beam resonance. In addition, the pattern at the first space aliasing beam mode is found to be located at high $|\vec{k}|$ values that are far away from the interested physics. For the spectral solver the numerical Cerenkov instability of the first aliased beam mode is located at a predicted pattern in $\vec{k}$ space so it can be conveniently eliminated by applying simple filters directly in $\vec{k}$ space.

We developed a fully parallelized three-dimensional electromagnetic spectral PIC code called UPIC-EMMA that was built using components of the UCLA PIC Framework called UPIC [11]. A spectral EM-PIC code has the same basic flow chart as a finite-difference-time-domain (FDTD) PIC code. In a spectral EM-PIC code both the charge and current are deposited on the mesh from the particles; the forces exerted on the particles are interpolated from the mesh points, and particles are advanced using the Lorentz forces. The main difference between the spectral PIC code and FDTD PIC code is the solver used to advance the electromagnetic field and that all field quantities, including the charge and current densities, are defined at the same locations on a cell (no Yee mesh [12] is needed). In a spectral PIC code the charge and current are directly deposited, and a strict charge conserving current deposit is not needed because Gauss's law is solved at each time step using the charge density.

There are no dispersion errors for light waves due to the grid (however there are errors from the finite time step). This is a significant advantage of the spectral solver, whereas a FDTD code describes the $[k]_i$ operator to $\mathcal{O}(k_i \Delta x_i)^3$, the spectral code has no errors in the finite $[\vec{k}]$ operator. In addition, when including time step errors, the numerical dispersion of a spectral PIC code is super-luminal, while that of the FDTD code is sub-luminal. The more accurate and superluminal aspect of the EM dispersion relation provided by the spectral solver (together with the simple filters) is crucial for eliminating the numerical Cerenkov instability. This ensures no non-physical interaction between waves and particles in the first Brillouin zone for the spectral PIC code.

---

* tpc02@ucla.edu

03 Alternative Acceleration Schemes

A23 - Laser-driven Plasma Acceleration

LAUNCHING LASER AND ELECTRON BEAM

To model LWFA stages including beam loading it is necessary to have an antenna and a cathode in the boosted frame. Next, we discuss how these are implemented in UPIC-EMMA.

Moving Antenna

As discussed in [3] and [13], the effective spot size of the laser increases by a factor of $\gamma_b^2(1 + \beta_b)$ because the Rayleigh length of the laser contracts by γ_b and the pulse length expands by $\gamma_b(1+\beta_b)$. To prevent the need for using a simulation box with transverse size $\sim \gamma_b^2$ times that is needed in the lab frame, we utilize a thin slice of grids at the plasma boundary as an antenna to drive the laser pulse into the plasma. The antenna moves backward together with the plasma boundary in the boosted frame.

In the spectral code, the transverse and longitudinal components of the fields are solved for separately. Therefore, on the antenna we set ρ equal to zero so there are no longitudinal fields on it. When launching a laser from the antenna, we assign current (in the direction of the laser polarization direction) at every point inside the antenna such that $\vec{E}$ has the desired form and polarization. The other components and the magnetic field follow naturally from Maxwell equations. The antenna has a finite width of around $\lambda/2$ where λ is the wavelength of the laser in vacuum to eliminate any backward propagating signal. The current for generating the laser is added after the current is deposited for all the particles in the system is finished.

Beam Cathode

Similarly to the initialization of laser, when initializing a particle beam in the Lorentz boosted frame the effective β^* contracts, which greatly enhances the effective spot sizes of the beam. We implement a beam cathode in UPIC-EMMA which, similarly to the moving antenna for laser, launches beam particles from a thin slice moving together with the plasma boundary. The corresponding EM fields produced by the beam are likewise initialized within the slice. The beam cathode also enables UPIC-EMMA to be used to simulate loading a particle beam into a wake driven by a laser and simulate plasma wakefield acceleration (PWFA).

BENCHMARK WITH OSIRIS

To benchmark the boosted frame simulation results from UPIC-EMMA, we performed extensive simulations. Here we present simulations of a 1 GeV LWFA stage with both UPIC-EMMA in a boosted frame and OSIRIS [14] in the lab frame. OSIRIS uses a FDTD solver, e.g. Yee solver, to push the EM field. The parameters for the OSIRIS simulations are listed in table 1, and the results for the $a_0 = 8.0$ cases are shown in figure 1. From the plasma density plot and wakefield plot in the Lorentz boosted frame, we can see clean physical results with no evidence of the numerical Cerenkov instability. Good agreement for the on-axis

Table 1: Simulation Parameters for the Simulations Shown in Figure 1 and 2 – ω_0 is the Laser Frequency and k_0 is the Laser Wave Number in the Lab Frame

2D LWFA boosted frame simulation	
Plasma	
plasma column length L	0.9 cm
density n_0	2×10^{18} cm^{-3}
Laser	
pulse length τ	30 fs
norm. vector potential	$a_0 = 8.0$
pulse waist W	15 μm
Simulation	
grid size $(k_0\Delta x_1, k_0\Delta x_2)$	(0.0982, 0.0982)
time step $\omega_0\Delta t$	0.0225
number of grid in box	16384×512
boosted frame γ_b	14
particle shape	quadratic
3D PWFA lab frame simulation	
Plasma density n_0	5×10^{16} cm^{-3}
Beam	
pulse length τ	113.7 fs
spot size W	10 μm
beam energy	22.5 GeV

wakefield is found between OSIRIS lab frame and UPIC-EMMA boosted frame simulation. More comparisons can be found in Ref. [15].
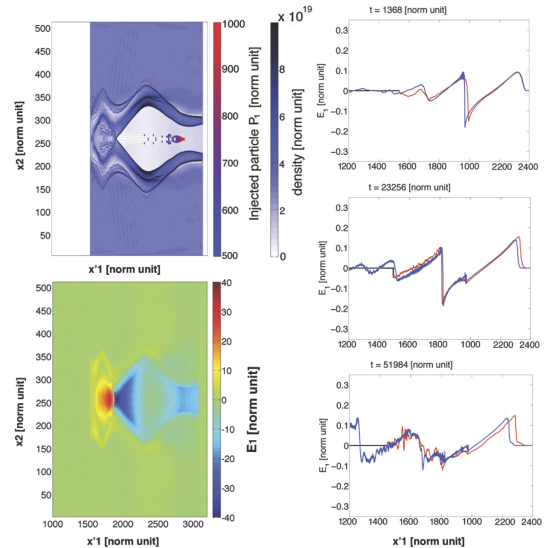
Figure 1: Highly nonlinear case at $a_0 = 8.0$. Left column shows the 2D plots of plasma electron density, and the corresponding E_1 at $t = 221$ [norm unit] in the boosted frame ($\gamma_b = 14$). The second column shows the on-axis E_1 comparison between OSIRIS lab frame, and UPIC-EMMA boosted frame simulation ($\gamma_b = 14$).

BOUNDARY CONDITIONS

Currently, in UPIC-EMMA there are 3 types of EM boundary conditions (b.c.) available: (i) 3D periodic boundary; (ii) 3D conducting boundary; and (iii) mixing boundaries with conducting boundary in x_1 and x_2, and periodic boundary in x_3. The particles are specularly reflected from the conducting boundary. The conducting b.c. is particularly useful when modeling beam loading or PWFA. This is due to the fact that when all the three directions are periodic, the charge neutrality in the simulation box is enforced, while in the PWFA simulation the system is non-neutral because of the electron beam. To illustrate this issue we show UPIC-EMMA results from a lab frame simulation where only one driving particle beam is modeled (no trailing beam). In figure 2 we present the results of a 3D PWFA simulation in the lab frame, using 3D periodic b.c. (first row), and mixing b.c. (second row), and the comparison in the on-axis wakefields are shown in figure 2 (c) and (d). The QUICKPIC results are also shown in figure 2 (c). In figure 2 (d) we plot the transverse lineout of the wakefield in the bubble, to illustrate the differences in the wakefield due to the different b.c.
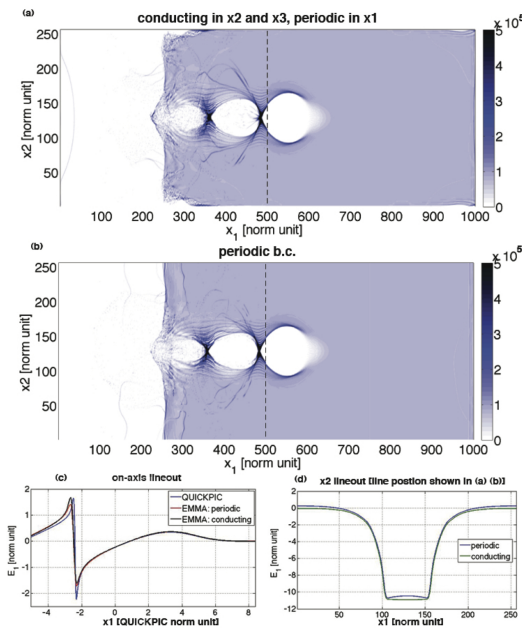
Figure 2: (a) and (b) show the 2D plasma density plot of a 3D PWFA lab frame simulation using the parameters shown in table 1. (a) uses the conducting b.c. in the transverse directions of the propagating driving beam, while (b) uses 3D periodic b.c. In (c) the on-axis wakefields are compared between the mixing b.c. and 3D periodic b.c., and also compared with the QUICKPIC results. In (d) we plot the transverse lineout of the wakefield in the bubble for the two types of b.c; the position of this cross section is shown in (a) and (b).

CONCLUSIONS

In this paper we briefly described a new simulation code called UPIC-EMMA that can model LWFA stages, including beam loading from an injected particle beam, at very high gammas γ_b. UPIC-EMMA uses a spectral solver to mitigate the numerical instability induced by the relativistic plasma drift. The spectral solver together with a band-pass filter conveniently mitigates the numerical instability.

We have also implemented a moving antenna to launch a laser and a moving cathode to launch a particle beam. The moving cathode allows beam loading as well as PWFA studies. The implementation of a mixing boundary condition is shown to give correct results for the wakes from the driving particle beams.

We presented details of LWFA parameters for simulating LFWA stages using UPIC-EMMA in the Lorentz boosted frame. The γ_b of the boosted frame is chosen such that the laser frequency is in the same order as the plasma frequency so neither of these two characteristic lengths are over-resolved. We compared the transformed boosted frame data in UPIC-EMMA with the lab frame data from OSIRIS, and good agreements are found.

REFERENCES

[1] T. Tajima, J. M. Dawson, Phys. Rev. Lett. 43, 267 (1979).

[2] J. -L. Vay, Phys. Rev. Lett. 98, 130405 (2007)

[3] S. F. Martins, R. A. Fonseca, L. O. Silva, W. Lu, W. B. Mori, Comp. Phys. Comm. 181, 869 (2010).

[4] J. -L. Vay, C. G. R. Geddes, E. Cormier-Michel, D. P. Grote, J. Comp. Phys. 230, 5908 (2011).

[5] C. D. Decker, W. B. Mori, Phys. Rev. Lett., Vol. 72, 490 (1994)

[6] B. B. Godfrey, J. Comp. Phys. 15, 504 (1974); B. B. Godfrey, J. Comp. Phys. 19, 58 (1975)

[7] K. Nagata, PhD thesis, Osaka University, 2008.

[8] P. Yu et.al, in Proc. 15th Advanced Accelerator Concepts Workshop, Austin, TX, 2012.

[9] B. B. Godfrey and J.-L. Vay, J. Comp. Phys., 248, 33-46 (2013)

[10] X. Xu, et. al., Comp. Phys. Comm., Vol. 184, 2503–2514 (2013)

[11] V. K. Decyk, Comp. Phys. Comm. 177, 95 (2007).

[12] K. Yee, IEEE Transactions on Antennas and Propagation, Vol. 14, 302 (1966)

[13] J.-L. Vay, C. G. R. Geddes, E. Cormier-Michel, D. P. Grote, arXiv:1009.2727v2

[14] R. A. Fonseca, et al., in: P.M.A. Sloot, et al. (Eds.), ICCS, in: LNCS, Vol. 2331, 2002, pp. 342–351.

[15] P. Yu et. al. in preparation.